International Journal of Biological Macromolecules 268 (2024) 131939

Contents lists available at ScienceDirect

International Journal of Biological Macromolecules

journal homepage: www.elsevier.com/locate/ijbiomac

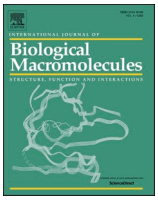

Immobilization of human tyrosine hydroxylase onto magnetic nanoparticles – A novel formulation of a therapeutic enzyme☆

Zsófia Molnár[a,b], Gábor Koplányi[a], Réka Farkas[a], Noémi Péli[a], Balázs Kenéz[a], Balázs Decsi[c], Gábor Katona[d], György T. Balogh[c,e], Beáta G. Vértessy[b,f], Diána Balogh-Weiser[a,g,*]

[a] Department of Organic Chemistry and Technology, Faculty of Chemical Technology and Biotechnology, Budapest University of Technology and Economics, Műegyetem rkp. 3., H-1111 Budapest, Hungary
[b] Institue of Enzymology, Research Center of Natural Science, Eötvös Loránd Research Network, Magyar tudósok körútja 2., H-1117 Budapest, Hungary
[c] Department of Chemical and Environmental Process Engineering, Faculty of Chemical Technology and Biotechnology, Budapest University of Technology and Economics, Műegyetem rkp. 3., H-1111 Budapest, Hungary
[d] Institute of Pharmaceutical Technology and Regulatory Affairs, Faculty of Pharmacy, University of Szeged, Eötvös u. 6, H-6720 Szeged, Hungary
[e] Department of Pharmaceutical Chemistry, Semmelweis University, Hőgyes E. Street 7–9, H-1092 Budapest, Hungary
[f] Department Applied Biotechnology and Food Science, Faculty of Chemical Technology and Biotechnology, Budapest University of Technology and Economics, Műegyetem rkp. 3., H-1111 Budapest, Hungary
[g] Department of Physical Chemistry and Materials Science, Faculty of Chemical Technology and Biotechnology, Budapest University of Technology and Economics, Műegyetem rkp. 3., H-1111 Budapest, Hungary

ARTICLE INFO

Keywords:
Tyrosine hydroxylase
Magnetic nanoparticles
Catalytic activity
Enzyme immobilization
Physico-chemical characterization

ABSTRACT

Human tyrosine hydroxylase (hTH) has key role in the production of catecholamine neurotransmitters. The structure, function and regulation of hTH has been extensively researched area and the possibility of enzyme replacement therapy (ERT) involving hTH through nanocarriers has been raised as well. However, our understanding on how hTH may interact with nanocarriers is still lacking. In this work, we attempted to investigate the immobilization of hTH on magnetic nanoparticles (MNPs) with various surface linkers in quantitative and mechanistic detail. Our results showed that the activity of hTH was retained after immobilization via secondary and covalent interactions as well. The colloidal stability of hTH could be also enhanced proved by Dynamic light scattering and Zeta potential analysis and a homogenous enzyme layer could be achieved, which was investigated by Raman mapping. The covalent attachment of hTH on MNPs via aldehyde or epoxy linkers provide irreversible immobilization and 38.1 % and 16.5 % recovery (ER). The hTH-MNPs catalyst had 25 % ER in average in simulated nasal electrolyte solution (SNES). This outcome highlights the relevance of immobilization applying MNPs as a potential formulation tool of sensitive therapeutic enzymes offering new opportunities for ERT related to neurodegenerative disorders.

1. Introduction

Tyrosine hydroxylase (hTH) catalyzes the hydroxylation of L-Tyr to L-3,4-dihydroxyphenilalanine (L-DOPA), playing a crucial role in the production of neurotransmitters in both vertebrates and invertebrates [1]. Regarding its catalytic properties, TH is a non-heme iron containing aromatic amino acid hydroxylase (also referred to as tyrosine 3-monooxygenase, E.C. 1.14.16.2), that uses (6*R*)-L-erythro-5,6,7,8-tetrahydrobiopterin (BH_4) cofactor for the incorporation of molecular oxygen during the reaction [2]. Besides its physiological importance, biocatalytic application of TH was reported as well, for example in the cell-free synthesis of dopamine [3], and in metabolic engineered strains for hydroxytyrosol [4] or alkaloid production [5]. TH is a homotetrameric enzyme with each monomer consisting of an *N*-terminal

☆ BRIEFS. Immobilization of human tyrosine hydroxylase (hTH) on magnetic nanoparticles (MNP) with various surface modifications was investigated. Several immobilization strategies were explored, such as adsorption, electrostatic interaction, and covalent attachment. The enzymatic activity of hTH was retained after immobilization. This study is an example how interactions between carrier surface and structural features of a protein can enhance immobilization and stabilization.

* Corresponding author at: Department of Organic Chemistry and Technology, Faculty of Chemical Technology and Biotechnology, Budapest University of Technology and Economics, Műegyetem rkp. 3., H-1111 Budapest, Hungary.
E-mail address: balogh.weiser.diana@vbk.bme.hu (D. Balogh-Weiser).

https://doi.org/10.1016/j.ijbiomac.2024.131939
Received 27 September 2023; Received in revised form 17 April 2024; Accepted 26 April 2024
Available online 29 April 2024

regulatory, a middle catalytic, and a C-terminal tetramerization domain [6]. The regulation [7–9], structure [6,10] and mechanism [2,11,12] of human TH (hTH) has been widely studied, especially in relation to neurodegenerative diseases. Biallelic hTH deficiency can cause severe dystonia in individuals [13], and the dysfunction of hTH has been associated with Parkinson's disease as well [14]. These diseases have been targeted with different therapeutic strategies such as the administration of L-DOPA together with carbidopa to prevent its peripheral metabolism [15], but these can have serious side effects and are not applicable in all cases [16,17]. This calls for further research into the function of hTH and for additional therapeutic solutions.

Investigations into a potential enzyme replacement therapy of hTH have been already conducted [15,18]. In one work of *Bezem* et al., hTH was stabilized in maltodextrin nanoparticles that were successfully delivered to neuronal cells [19]. In another work of the same group, adsorption aided by electrostatic interactions on porous silica nanoparticles was explored as a promising nanocarrier system for enzyme delivery through the blood brain barrier (BBB) [20]. These two studies showed that hTH can be stabilized and delivered in its active form with different nanocarriers. In this study, our aim was to further investigate this phenomenon with the immobilization of hTH on magnetic nanoparticles (MNPs). Among nanocarriers, MNPs could provide unique possibilities for the investigation of enzyme immobilization due to their extremely rapid and mild separation by magnetic forces and their fine-tunable surface properties allows the optimization of enzyme binding [21]. Among the family of metal-oxide nanoparticles, the magnetite-based MNPs (Fe_3O_4) are one of the most widely-used solid supports owing to the high chemical and mechanical resistance, biocompatibility, fine-tunable surface and their ferromagnetic properties [22]. After the proper surface modification, MNPs are capable of immobilizing enzymes, cells and other proteins on their surface and they can be used for any further purposes [23]. Thanks to their exceptional advantages, the application spectra of MNPs as solid support is really extensive in the fields of nano-biotechnology [24], enzyme immobilization [21], biomedical applications [25], food industry [26] and biosensors [27]. Recently, it has been demonstrated that a magnetic field applied externally can mediate the capacity of magnetic nanoparticles to permeate the blood-brain barrier. This breakthrough greatly augments the potential of MNPs applications [28–32]. A further benefit of the application of MNPs in such therapies is that their absorption and delivery can be controlled more firmly than in the case of other nanocarriers [33]. For hTH, its activity is significant in the central neuronal system and the adrenal glands [34,35]. Controlled targeting can lower the impact of side effects of the enzyme substitution therapy. In addition, the rapid preliminary investigation about enzymatic binding on MNPs could also be adopted to other carriers such as silica nanoparticles commonly used in drug delivery, since the optimization of the functional groups on the MNPs surface (especially in case of MNPs with silica coating) could be easily mimicked.

In this work, we aimed to investigate a wider scope of immobilization strategies for hTH, which has not yet been addressed in the literature. In addition, the immobilization of hTH applying MNPs and the comprehensive investigation of immobilizates involving colloidal, structural and enzymatic investigations has also not been reported before. Thus, the adsorptive, ionic and covalent immobilization of hTH was carried out on MNPs with different surface modifications. Unmodified MNPs and MNPs covered with silica-shell were expected to adsorb hTH on their surface; amino-functionalized (MNP—Am) was investigated as a nanocarrier suitable for ionic interactions; and MNPs additionally surface-modified on primer amino-groups of MNP-Am with glutaraldehyde (GA) and glycerol diglycidyl ether (GE) were tested as nanoparticles capable of forming covalent attachment with hTH. Different temperatures (4, 25 and 37 °C) were tested during the immobilization process to evaluate its effect on the stability of the immobilized hTH involving Zeta potential and Dyanmic Light Scattering (DLS) measurements. The catalytic activity of the immobilized hTH was tested and compared under standard conditions and in nasal electrolyte solution (SNES). Furthermore, we investigated the surface distribution of the surface modifying groups and the immobilized hTH with Raman mapping as well.

2. Methods

2.1. Materials

All solvents used in this study were of analytical grade. Ethanol (EtOH), 2-propanol (IPA) are the products of Molar Chemicals Ltd. (Halásztelek, Hungary), and ethylene glycol, acetic acid, were purchased from Merck Ltd. (Budapest, Hungary). Water was obtained from a Milli-Q water-purification system (Millipore, Bedford, MA, USA) and applied for the preparation of all aqueous solutions. Sodium chloride (NaCl), calcium chloride ($CaCl_2$, anhydrous), potassium chloride (KCl) 4-(2-hydroxyethyl)-1-piperazineethanesulfonic acid) (HEPES), ammonia solution (35 % aqueous solution) sodium acetate trihydrate, polyethylene glycol 400 (PEG 400), polyethylene glycol 4000 (PEG 4000, Mw = 4 kDa), tetraetoxysilane (TEOS), 3-aminopropyltrimethoxysilane, glutardialdehyde (GA, 25 % aq. solution), glyceroldiglycidylether (GE), tryptone, yeast extract, isopropyl-β-D-thiogalactoside (IPTG), Glutathione Sepharose 4B GST-tagged protein purification resin was purchased CytivaTM (GST-resin), glutathione (GSH), 6,7-dimethyl-5,6,7,8-tetrahydropterin cofactor-analogue ($DMPH_4$), L-tyrosine (L-Tyr), L-3,4-dihydroxyphenylalanine (L-DOPA), sodium periodate ($NaIO_4$), iron(*II*)sulphate ($FeSO_4$), iron(*III*)chloride-hexahydrate, catalase and bovine serum albumin (BSA) was obtained from Sigma-Aldrich Ltd. (St. Luis, MO, USA). Tobacco Etch Virus (TEV) protease was expressed and purified in our laboratory.

2.2. Production of native human tyrosine hydroxylase (hTH)

The production of hTH was carried out in *E. coli* BL21 cells with GST fusion tag, for details, see Supplementary Information (SI), Section 1. *Protein Expression and Purification*. The efficiency of protein purification is shown in Fig.S1 of SI.

2.3. Characterization of native hTH

The characterization of native hTH applying Dynamic Light Scattering and Zeta-potential analysis is described in SI, Section 3.3. *Dynamic Light Scattering and Zeta Potential Measurements*. The enzyme activity assays are presented in Section 4. *Investigation of enzymatic activity of hTH*. The details about structural evaluation of native protein are given in Section 5. *Software and scripts used for the prediction of physico-chemical parameters and protein visualization* in SI.

2.4. Synthesis, surface modification of and characterization of magnetic nanoparticles

The synthesis and surface modification of the applied MNPs carriers was done in our laboratory, for details see SI Section 2. *Synthesis and surface modification of magnetic nanoparticles,* Section 3. *Characterization of surface modified magnetic nanoparticles and hTH immobilized on magnetic nanoparticles,* and Section 5. *Software and scripts used for the prediction of physico-chemical parameters and protein visualization.*

2.5. Immobilization of hTH on MNPs

The immobilization of hTH was carried out in screw-capped 4 mL vials. 3.0 mg MNPs carriers were sonicated in 925 μL HEPES buffer (10 mM, pH 6.8) for 10 min at 35 kHz, 160 W at room temperature in US bath (Sonorex Digitec DT255 US bath, Bandelin Gmbh, Berlin, Germany). The purified hTH solutions were defrosted right before use and kept on ice during the experiments. Then 75 μL of purified hTH solution

(2.2 mg mL^{-1}, 10 mM HEPES, pH 6.8) was added to each MNPs carrier suspension and shaken at 600 rpm applying orbital shaker at various temperature (4 °C, 25 °C and 37 °C), Vibramax 100, Heidolph Gmbh, Schwabach, Germany), for 60 min followed by the isolation by using permanent neodymium magnets (N35). After the magnetic isolation, samples (3 μL, each) were taken from the binding supernatant and the absorbance of the samples was measured at 280 nm by ThermoScientific™ NanoDrop2000 spectrophotometer (Thermo Fisher Scientific Inc., Waltham, MA, USA) using Protein A280 method. Protein concentration in samples was measured with the application of extinction coefficient for hTH (40,340 M^{-1} cm^{-1}). To characterize the efficiency of the immobilization, the immobilization yield (Y_I) was determined using the formula $Y_I = c_I \times c_0^{-1}$, where c_I [mg mL^{-1}] is the measured hTH concentration in the binding supernatant, and c_0 [mg mL^{-1}] is the initial hTH concentration in the binding solution. Finally, the MNP-hTH biocatalysts were washed with HEPES buffer (1 mL, 10 mM, pH 6.8), the particles were separated permanent using a neodymium magnet (N35) and were tested directly in the enzymatic activity assay. For enzyme leaching tests, MNPs (3.0 mg) were suspended in HEPES buffer (1.0 mL HEPES buffer, 10 mM, pH 6.8) using orbital shaker at 750 rpm (Vibramax 100, Heidolph Gmbh, Schwabach, Germany) for 60 min then particles were separated using a neodymium magnet (N35). The protein content of residual supernatant was measured by a ThermoScientific™ NanoDrop2000 spectrophotometer as it described above.

2.6. Enzyme activity assay

For the spectrophotometric activity assay, the method of Vermeer et al. [36] was adapted, which is based on the oxidation of L-DOPA to dopachrome, a compound with an absorbance maximum at 475 nm. For the activity measurement of the native hTH enzyme, 0.01 mg mL^{-1} hTH, 100 μM L-Tyr, 50 μM Fe_2SO_4, 200 μM $NaIO_4$, and 0.1 mg mL^{-1} catalase were mixed in HEPES buffer (1 mL, 10 mM, pH 6.8), then the reaction was started with the addition of 0.25 mM 6,7-dimethyl-5,6,7,8-tetrahydropterine hydrochloride ($DMPH_4$), which is the non-natural cofactor of hTH. Measurements were conducted in 96-well half-area plates in a Thermo Scientific™ Multiskan SkyHigh Microplate Spectrophotometer (Thermo Fisher Scientific Inc., Waltham, MA, USA). Absorbance was monitored at 475 nm for 30 min at 4 °C, 25 °C or 37 °C. For the activity measurement of the immobilized enzymes, the same reaction components (L-Tyr, Fe_2SO_4, $NaIO_4$, catalase, $DMPH_4$) in the same final concentrations were mixed with 3 mg of immobilized enzyme in screw-capped 4 mL vials, which was shaken at 600 rpm by an orbital shaker (Vibramax 100, Heidolph Gmbh, Schwabach, Germany) to keep the nanoparticles in suspension. Samples were taken after 15 min for spectrophotometric measurement at 475 nm. For every measurement, blank samples were prepared with the same method with MNPs that did not contain immobilized enzyme. Production of L-DOPA was determined using a molar extinction coefficient for dopachrome of $\varepsilon = 1980$ M^{-1} cm^{-1} at wavelength at 475 nm, 37 °C.

Based on the UV–Vis measurement, the specific enzymatic activity (U_E) was determined using the formula: $U_E = n_P \times (t \times m_E)^{-1}$, where n_P [μmol] is the amount of the product, t [h] is the reaction time, m_E [g] is the mass of the enzyme in the immobilized system.

3. Results and discussion

3.1. Physico-chemical characterization of hTH indicates formation of stable colloids

The physico-chemical properties of proteins strongly influence their behavior and stability in different media. Generally, protein aggregation can occur during improper folding or if the conformational changes of the folded protein expose their hydrophobic amino acid residues or regions that are otherwise deeply buried in the native state [37]. Aggregation is primarily driven by hydrophobic forces that can result in the formation of amorphous aggregates, oligomers or in some special cases, amyloid fibrils [38]. Zeta potential (Z) indicates the stability of a colloidal system and can be used to characterize the electrokinetic stability, which may refers to the process of protein aggregation in solution. However, it needs to be noted that Zeta potential is only one the parameters which could affect on the stability of a colloidal systems, since secondary interactions, steric and osmotic effects should also be taken into account. It has already been reported in numerous cases [20,39,40] that hTH is prone to aggregation, which could influence the enzyme activity and the further biocatalytic applications. We investigated the Zeta potential of hTH in solution at different temperatures (T = 4 °C, 25 °C and 37 °C) as described in ESI Section 5. There was no significant change in the Zeta potential during the one-hour incubation of hTH solutions at different temperatures, Zeta potential on Fig. 1A. Values indicated good electrokinetic stability, since they ranged between −15 and −20 mV, which is far enough from the critical range usually associated with aggregation($-5 < Z > +5$ mV) [41].

Protein aggregation can be directly studied via dynamic light scattering (DLS), as well, as the size distribution of the protein particles can provide information on the molecular assembly processes present in the solution. Despite that Z values suggest good electrokinetic stability, DLS measurements of the same native hTH samples shows that aggregation occurs at all three tested temperatures in the observed one-hour time frame (Fig. 1B,C and D). At 37 °C, the starting point shows that a notable portion of the enzyme is already aggregated. Aggregation progresses at lower temperatures (Fig. 1B,C), nonetheless. These results indicate that electrokinetic stability itself is not enough to keep hTH in its soluble single enzyme form, the formation of aggregates advanced in the investigated condition. The fact that Zeta potential did not change in the observed one-hour timeframe the process suggests that non-electrostatic interactions are not the decisive parameters in the protein aggregation. Based on the Z values and DLS curves it can be said, that forming protein aggregates are stable and suitable for functional immobilization.

3.2. Characterization of magnetic nanoparticles with different surface linkers

One of the most often mentioned advantage of the immobilization strategies is that a properly chosen and optimized immobilization method can increase the stability of an enzyme [42]. In this work, we aimed to investigate the effect of the surface properties of the carrier and the immobilization method on the stability and activity of hTH. We chose MNPs as a carrier, as it is versatile and can be easily sedimented with the use of permanent magnets. Immobilization of hTH on MNPs carriers has not yet been reported in the literature, increasing the significance of our present study. Synthesis and surface modifications of MNPs were carried out in our laboratory. We performed the immobilizations on five types of MNP carriers with different surface properties showed on Fig. 2, Panel A: bare MNPs particles (MNP), MNPs covered with silica shell (MNP—Si), MNPs further functionalized with amino groups (MNP—Am), and MNPs additionally surface modified with either glutardialdehyde (MNP-GA) or glycerol diglycidyl ether (MNP-GE). Regarding the immobilization mechanism (Fig. 2 Panel B), MNP and MNP-Si and MNP-Am are suitable for physical binding of hTH. The MNP and MNP-Si carriers have negative charges on their surface, allowing slight ionic interaction with the positively charged protein region. In case of MNP—Si, ethoxy-chains as residues of TEOS precursor could form hydrophobic interactions as well (indicated with yellow satire on Fig. 2B at MNP—Si). The free amino groups of MNP-Am representing positive charge are capable of ionic interaction with the negative sites of hTH. MNP-GA and MNP-GE have the potential for covalent attachment of proteins, because GA aldehyde linkers form Schiff-base with amino amin side chains, while GE epoxy linker also form covalent attachment in nucleophile substitution reaction type 2, (mostly with lysins, less with cysteine or serine due to their weaker nucleophilic character).

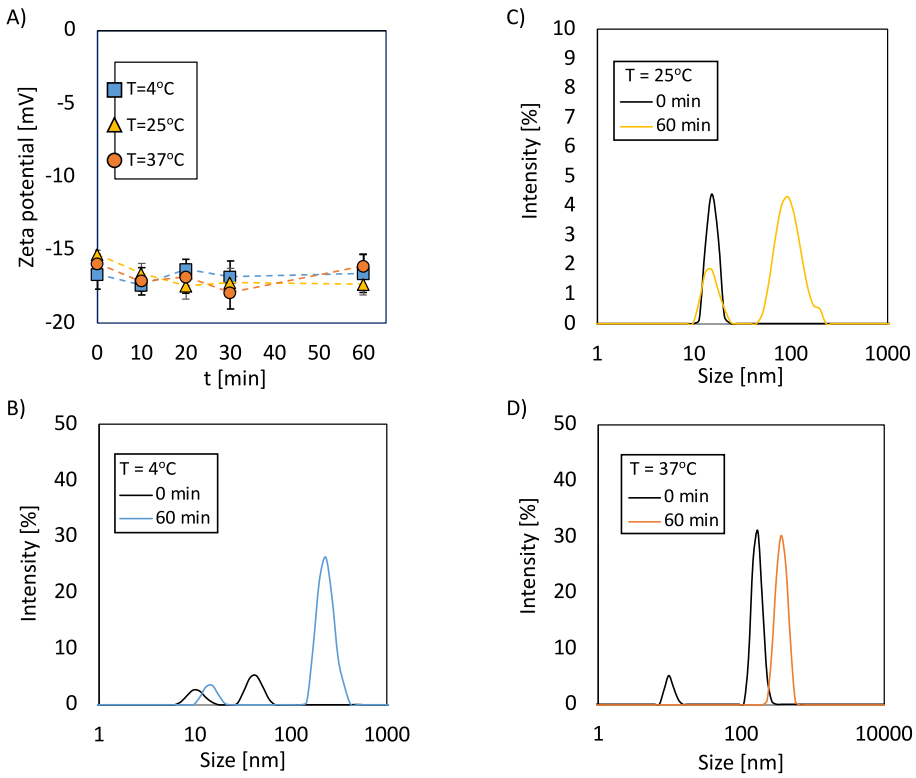

Fig. 1. Effect of the temperature (4 °C, 25 °C and 37 °C) on A) the Zeta potential of native (non-immobilized) hTH (0.165 mgmL^{-1}, in HEPES buffer 10 mM, pH 6.8) and on the size (diameter) distribution of native (non-immobilized) hTH in HEPES buffer (10 Mm, pH 6.8) at B) 4 °C, C) 25 °C and D) 37 °C in a one-hour time interval.

The particle size, morphology, elemental content and surface function groups of magnetic nanoparticles (MNP, MNP—Si, MNP—Am, MNP-GA and MNP-GE) were systematically investigated. Results of particle size distribution applying DLS (Fig. 3A) in accordance with Scanning Electron Microscope (SEM) images (see Fig.S2. in SI) showed that the typical size of bare MNPs is 596 ± 153 nm. MNPs after further modification such as silica-coating or functionalization with amino-silane and glutaraldehyde or glycerol diglycidyl ether are slightly larger than bare MNP (particle size of MNP-Si is 632 ± 208 nm, MNP-Am is 678 ± 156, MNP-GA is 632 ± 181 nm and MNP-GA is 603 ± 104 nm). It also needs to be noted that the difference in particle size between MNP and modified MNPs seems a bit larger on DLS curves, which could be explained by the increased solvate layer around the particles. The elemental analysis of MNP carriers was carried out using Energy Dispersive X-ray Analysis (EDX) coupled with SEM (Fig. 3B). Regarding the atomic percentage values (Atomic%), it can be observed that MNP contains C, Fe and O atoms and in case of MNP—Si, MNP—Am, MNP-GA and MNP-GE the presence of Si atom is obvious. In addition, the functionalization of the particles with amino-silane (3-aminopropyltrimtehoxysilane, ApTMOS see on Fig. 2.) causes slight increasing in Si content of the carrier (Si content given in Atomic% of the particles is 9.7 ± 1.4 %, 10.4 ± 0.8 % and 12.8 ± 0.7 % for MNP—Am, MNP-GA and MNP-GE respectively) compared to MNP-Si carrier (Si content given in Atomic% of the particles is 7.3 ± 0.7 %). The carbon and oxygen content of the samples is similar which could be explained by the fact that C and O atoms can come from organosilanes (TEOS or ApTMOS) and bifunctional linkers (GA or GE) and solvent residues, thus the differences in elemental content may blur. The presence of silica shell and modifier agents such as ApTMOS, GA or GE on MNP—Si, MNP—Am, MNP-GA and MNP-GE carriers are confirmed by Infrared Spectroscopy (IR) as well based on characteristic IR absorption wavelength (Fe_3O_4 at 560 cm^{-1}, Si–O–Si at 1070 cm^{-1}, C—H at 2900 and 3100 cm^{-1}, see on Fig.S3 in SI).

3.3. Immobilization of hTH onto magnetic nanoparticles with different surface linkers

Immobilization of hTH was carried out at 3 different temperatures, 4 °C, 25 °C and 37 °C to investigate the effect of the immobilization temperature on the stability of hTH. Immobilization yield (Y_I, %) based on the hTH concentration of binding buffers (amount of solubilized protein measured by Nanodrop system, see in SI Section 1) was defined to compare the immobilization ability of the carriers. As it can be seen on Fig. 4, temperature did not influence the immobilization yield, no trend could be inferred. It should also be noted that most immobilization studies are carried out at room temperature or higher, but in our case, lower temperatures did not hinder the immobilization process. This is a valuable information for the immobilization of sensitive enzymes. However, there were differences between the immobilization yields for the different types of carriers. MNP and MNP-Am carriers showed the highest immobilization yield, around 90 %. MNP-GA and MNP-GE, the carriers capable of covalent attachment were only able to bind around 65–80 % of the enzyme. The poorest performing carrier was the MNP—Si, in which case immobilization yield only reached about 60 %. It should be mentioned, that although the MNP carriers showed great immobilization yield, the particles were mostly aggregated at the end of the immobilization process, thus the unmodified carrier is not viable for further use.

The distribution of hTH on the surface of different MNP products was investigated by Raman chemical mapping (see the description in SI Section 3.4). To gain well distinguishable spectral difference between the poor Raman scatterer Fe_3O_4 MNPs and hTH laser irradiation induced phase transformation was applied. Relative high laser exposure (6 mW) of the magnetite nanoparticles can oxidize Fe_3O_4 into stable α-Fe_2O_3 via metastable γ-Fe_2O_3 as indicating the Raman peak at 1303 cm^{-1} attributed to the second order scattering of hematite as well as at 602, 493, 401, 286, 240 and 220 cm^{-1} corresponding to the vibration modes of

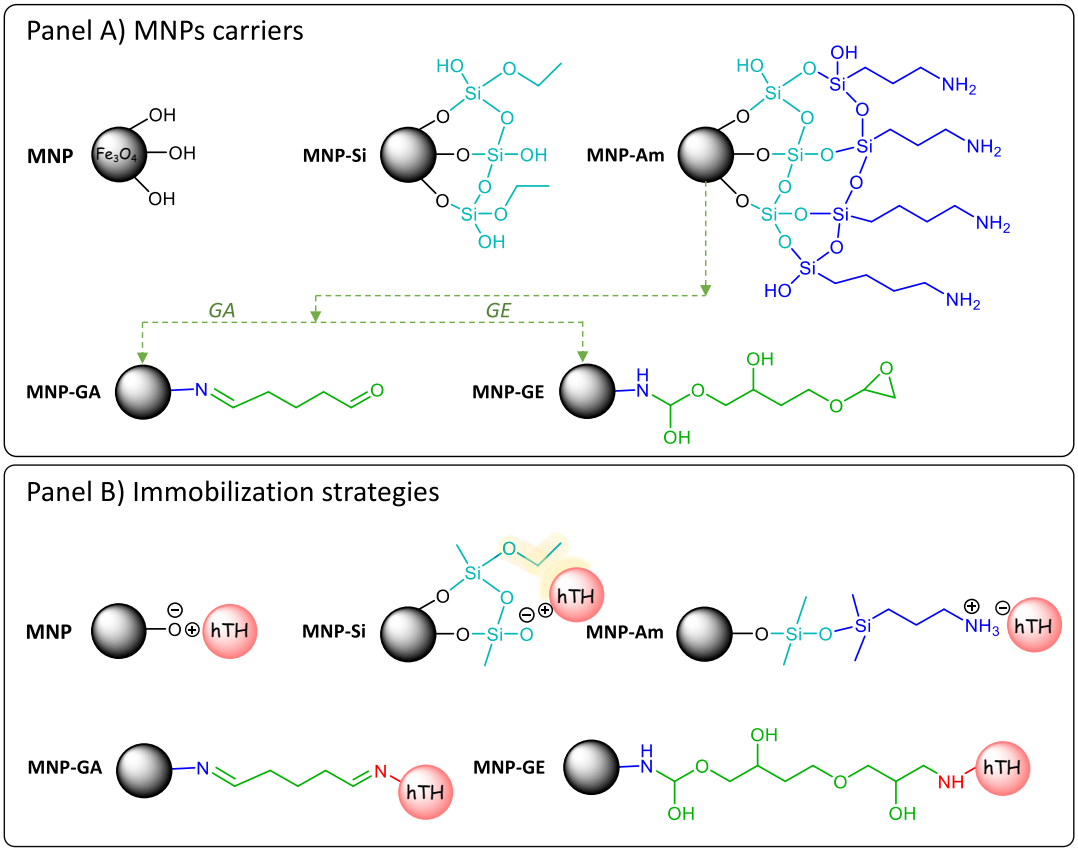

Fig. 2. Panel A) Surface modified MNPs carriers used in the study: Bare Fe_3O_4 (MNP), Bare MNP surface modifies with tetraethoxysilane (MNP—Si), MNP-Si further surface modified with 3-aminopropyl-trimethoxysilane (ApTMOS) (MNP—Am), MNP-Am further surface modified with glutardialdehyde (GA) (MNP-GA) and MNP-Am further surface modified with glycerol diglycidyl ether (GE) (MNP-GE), Panel B) strategies for the immobilization of hTH on to MNPs carriers.

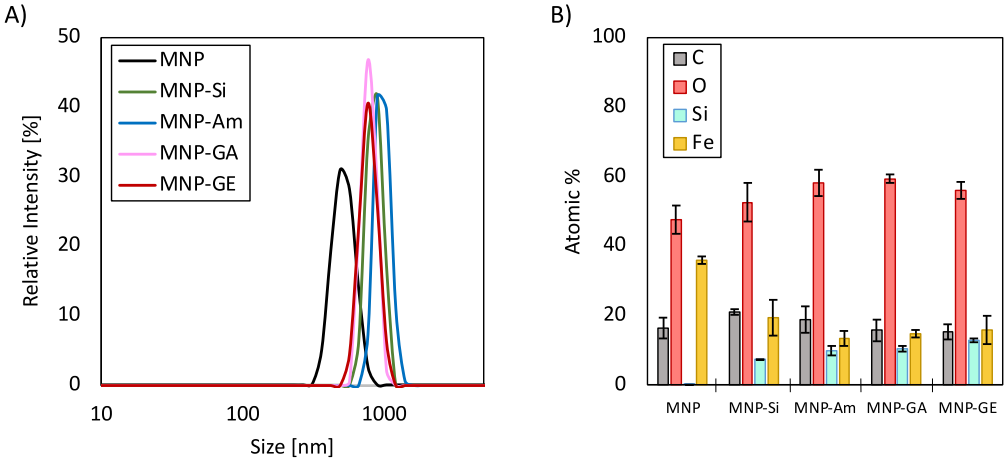

Fig. 3. Particle size distribution measured by DLS A) and element analysis applying SEM coupled EDX B) of different magnetic nanoparticles (MNP: bare Fe_3O_4 particles, MNP—Si: MNP covered with silica shell, MNP—Am: amino-functionalized MNP—Si, MNP-GA: glutardialdehyde functionalized MNP—Am, MNP-GE: glycerol diglycidyl ether functionalized MNP—Am).

Fe—O bonds [43]. For hTH, the amide I region (α-helix) was remarkable at 1664 cm^{-1}, this characteristic peak was selected for further profiling (Fig. S4, SI). After determination of spectral differences of MNP and hTH, Raman mapping was performed with the aim to investigate the distribution of hTH on the surface of different MNP carriers. The profiled Raman chemical maps of different MNPs were normalized to the frequency of occurrence of the selected spectral region (Fig. 5). The different colors of the chemical map represent the relative intensity change of hTH content on the surface of the MNP. Red color indicates its strong existence, the green area shows a mixed composition, whereas the blue color marks those regions of the map, whose spectral resolution contains different spectra, which is rather characteristic for MNPs. The relative intensity changes are in accordance with different hTH content. The results revealed that hTH formed a continuous coating on the surface of MNPs in case of each carrier, as shown by remarkably high relative intensity values between 0.5 and 0.75 (green and yellow color) on the Raman maps. The orange-red areas of Raman maps indicate some local maximum intensity values (~0.85) corresponding to sporadic

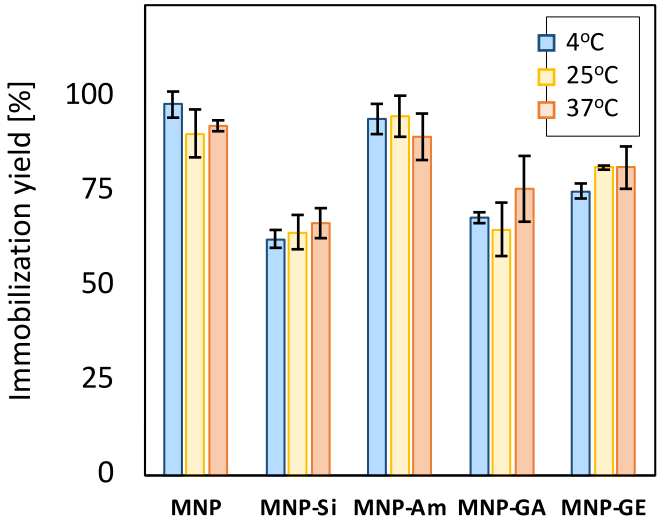

Fig. 4. Immobilization yield (Y_I, %) of hTH on different magnetic nanoparticles (MNP: bare Fe_3O_4 particles, MNP—Si: MNP covered with silica shell, MNP—Am: amino-functionalized MNP—Si, MNP-GA: glutardialdehyde functionalized MNP—Am, MNP-GE: glycerol diglycidyl ether functionalized MNP—Am) at ■ 4 °C, ■ 25 °C and ■ 37 °C. (For interpretation of the references to color in this figure legend, the reader is referred to the web version of this article.)

enriched hTH content on the MNP surface.

As all carriers were able to adequately immobilize hTH on their surface, we continued their characterization with the investigation of colloidal properties of the MNPs carriers before and after the immobilizations process by determing the Zeta potential values (Fig. 6). Firstly, it can be assessed that in all cases, the Zeta potential of the immobilized enzyme is higher than that of the native enzyme. The measured Zeta potentials were higher than that of the bare carriers, as well, except for MNP-GA and MNP-GE, the two carriers demonstrating covalent attachment. A possible explanation to this is that the immobilization is a reversible process for the first three carriers, enzymes can find a thermodynamically favorable position. For the covalent linkage, enzymes are irreversibly bound on the first instance a suitable amino acid residue (e.g. Lys) gets in the proximity of a reactive surface group. This orientation is not necessarily suitable or favorable for the thermodynamics of the system. The suspected difference between the binding ability of carriers was proved by enzyme leaching test, which showed that hTH could dissolve from the surface of MNP, MNP-Si and MNP-Am (enzyme leaching was 2.4 ± 0.8 % for MNP, 9.7 ± 4.0 % for MNP-Si and 6.5 ± 3.4 % for MNP—Am) but in case of MNP-GA and MNP-GE no solubized enzyme was observed after the washing test.

3.4. Enzymatic activity of hTH immobilized onto magnetic nanoparticles with different surface linkers

First, the specific enzyme activity (U_E, U g^{-1}) was determined for native hTH with different amount L-tyrosine as substrate (L-Tyr concentration was 50, 100 and 200 μM in the assays). Results showed that L-Try at 100 μM provided the highest U_E values ($U_E = 78.7 \pm 11.4$ U g^{-1} for 50 μM, $U_E = 136.4 \pm 7.5$ U g^{-1} for 100 μM and $U_E = 103.5 \pm 13.9$ U g^{-1} for 200 μM at 37 °C) thus 100 μM substrate amount was applied for all further investigations (see on Fig.S5 in SI). Next, we evaluated the activity of the hTH enzymes bound on the magnetic nanocarriers (MNP, MNP—Si, MNP—Am, MNP-GA and MNP-GE) to explore the possible effects of the different surfaces linkers of the carriers. As it can be seen from the results about immobilization yield and Zeta potential (Figs. 4 and 6), the function groups MNPs surface could affect the binding of hTH, thus it can influence the enzymatic activity as well. Native and immobilized hTH samples were parallelly investigated in the transformation of L-Tyrosine to L-DOPA followed by its oxidation to Dopachrome, which was analyzed by UV–Vis spectrophotometry. LC-MS measurements were also used to prove the L-DOPA formation directly (see Section 4.4. in SI Fig.S8–10). The specific enzymatic activity of native hTH was determined after incubating under the same conditions as the respective immobilized enzymes to serve as proper reference. Specific enzyme activity (U_E) of the native enzyme can be seen on Fig. 7. A), whereas the same results for the immobilized enzymes can be seen on Fig. 7. B). Interestingly, the native enzyme suffered a loss of activity after incubation at both 4 °C and 37 °C. Furthermore, it can be determined that the immobilized enzyme retained some of its activity in all case but also suffered a significant loss during the immobilization process. In two cases, for the carriers MNP-Am and MNP-GA immobilized at 25 °C, a higher amount of activity could be retained. We hypothesize that on the surface of MNP—Am, amino groups are in a protonated form on the pH of immobilization (pH 6.8). This can cause a mild ionic surface capable of interacting with the positive patches on the surface of hTH, enabling a gentle form of immobilization. This can be the reason for both the higher immobilization yields and the favorable retained activity. Interestingly, glutardialdehyde as covalent linker proved to be much better than glycerol diglycidyl ether despite achieving lower immobilization yields. The significance of the difference among the U_E values of immobilized hTH on MNPs was investigated by statistical analysis. The influence of carrier surface (bare MNP or MNP modified with Si, Am, GA, GE agents) and temperature (T) on U_E as the dependent variable was calculated. Statistical computations were conducted using the JASP software, with a sample size of $N = 3$ for all groups compared. Utilizing a two-way ANOVA analysis, we obtained significant results for both LQ and T, with p-values <0.001 and effect sizes (η2) of 0.286 and 0.273, respectively. Moreover, the interaction between LQ and T yielded a significant result ($p < 0.001$) with an η2 of 0.358, indicating that the combined effect of these factors significantly affects U_E. Assessment of homogeneity using Levene's test revealed non-significance ($p = 0.257$), suggesting uniform variances across groups. Post hoc analysis, employing Tukey correction, further elucidated the significance of temperature differences, with all pairwise comparisons showing $p <$ 0.001, as depicted on Figure7BF also visualizes significant deviations from the reference naked MNP at different temperatures, with asterisks indicating the significance levels (*$p < 0.05$, **$p < 0.01$, ***p < 0.001).

The physico-chemical properties of the different linkers found on the surface of a carrier is a key issue during enzyme immobilization, since not only the simple chemical functional groups can affect the carrier-enzyme interactions, but other parameters can have a role and synergic effect in the enzyme binding as well. Our approach was to characterize only the linker regions of the surface modification molecules, which are freely accessible to enzymes which allows the comparing the structural features of the linkers individually. In case of bare MNP there are no specific linkers on the surface. For MNP—Si, which stands for a silica shell covered MNP, ethoxy linkers could be present besides the silanol groups on the surface as well. Thus, for the comparison of relevant physico-chemical parameters of the linkers, aqueous solution of simple monosubstituted organosilane derivatives were used as model compound and parameters were determined using the Percepta program package of Advanced Chemistry Development, Inc. (ACD/Labs, Toronto, ON, Canada, see details is SI Section 5.), which is a widely used tool for the estimation of physico-chemical parameters in drug research (Table 1). The lipophilicity parameters (logP, logD) can be used to predict the lipophilic-lipophilic or dipole-dipole, while the pK_a can be applied to predict the contributions of ionic interactions between the linkers and the enzyme. The parameter n_{Rot} not only characterizes the degree of freedom of the linker, but also its length. Regarding the immobilization yield values, we must point out that among the individual linker-modified carriers (MNP—Si, —Am, -GA and -GE), the increased immobilization yield obtained in the case of MNP-Am due to the ionic nature of the chain-end primer amine since it is completely ionized at pH 6.8 based on the predicted pK_a value. In contrast, in case of

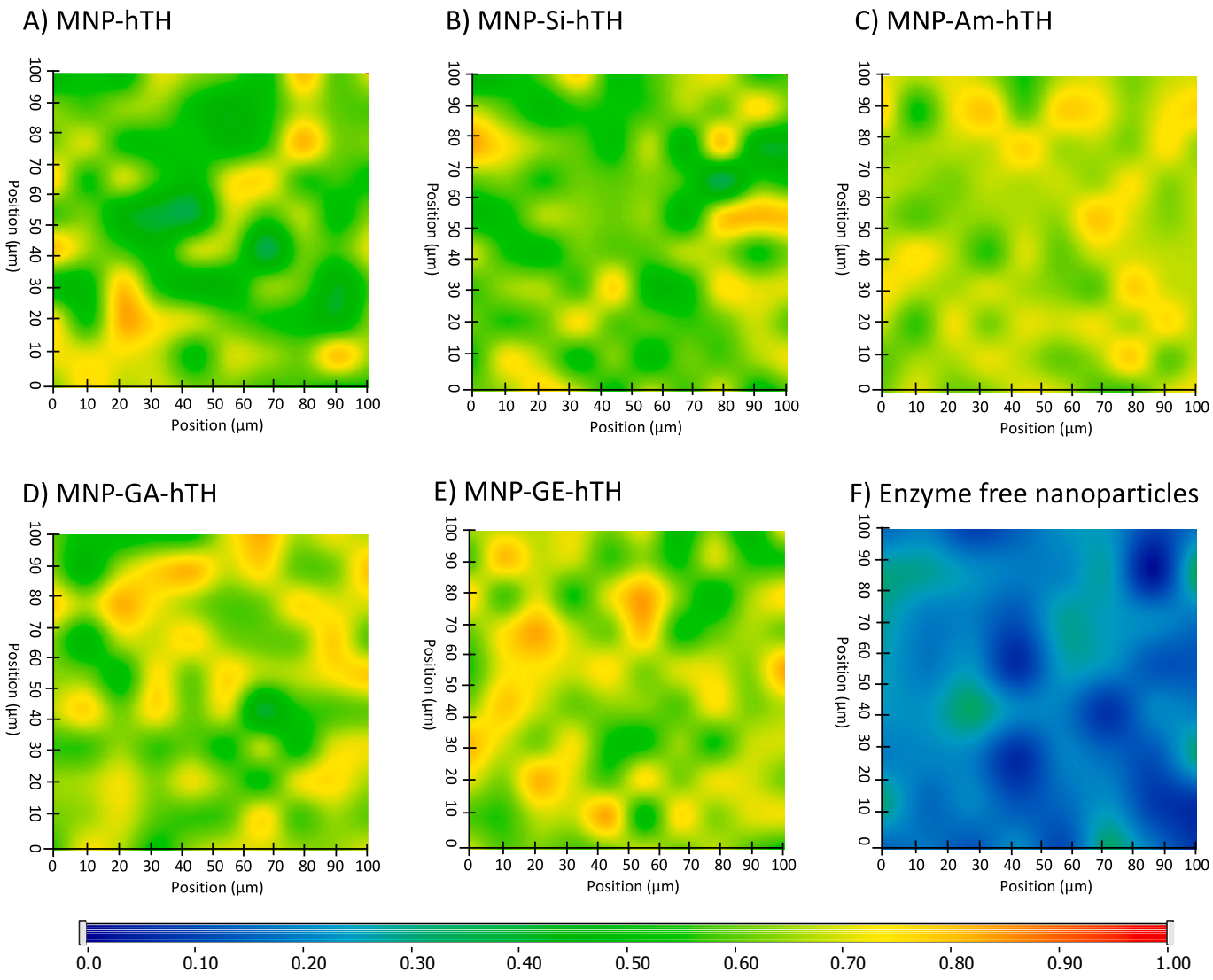

Fig. 5. Raman maps of hTH immobilized on different magnetic nanoparticles, A) MNP: bare Fe3O4 particles, B) MNP—Si: MNP covered with silica shell, C) MNP—Am: amino-functionalized MNP—Si, D) MNP-GA: glutardialdehyde functionalized MNP—Am, E) MNP-GE: glyceroldiglycidylether functionalized MNP—Am) and F) enzyme free initial magnetic nanoparticles: pooled samples of MNPs without enzyme, where the color scale indicates the presence of hTH (green, yellow, red, 0.5–0.85 on the scale) on the surface to hTH-free region (blue, 0.0 on the scale). (For interpretation of the references to color in this figure legend, the reader is referred to the web version of this article.)

MNP-GA and MNP-GE, secondary and tertiary amine groups with reduced basicity (lower pK_a, base) are present (more sterically closed), which is presumably less favorable in terms of enzyme fixation. Among the lipophilicity parameters related to the dipole-dipole interaction, a more significant difference could be identified in case of the pH-dependent partition coefficient ($logD_{pH6.8}$). Comparing the logD values of MNP-Si and MNP—Am, it clarifies that the increased lipophilicity does not favor the linker-enzyme interaction. In addition, the adverse effect of increased lipophilicity can also be attributed to the linkers responsible for covalent attachment, since even when examining the specific enzyme activity, the linker with reduced lipophilicity and correspondingly more polar (better solvated in an aqueous medium), MNP-GA, gave increased activity values compared to MNP-GE. Furthermore, MNP-Am with reduced lipophilicity was also outstanding in terms of enzyme binding efficiency and specific enzyme activity at 25 °C. It should be emphasized that, based on the temperature-dependent activity profiles of Fig. 7A and B, in the case of attachment to MNP—Am, the enzyme retained its native properties, which may be favorable from the point of view of general applications. Based on Table1, n_{Rot} and the increasing degrees of freedom of the linkers are believed to be unfavorable from the point of view of enzyme fixation, but the ionic and dipole interaction terms are likely to have a greater effect based on the results obtained.

The effects of the different immobilization methods can be reasoned by investigating the structural features of hTH, various visualizations of the tetrameric structure can be seen on Fig. 8. Fig. 8A shows the pattern of hydrophobic residues present on the surface, based on *Hagemans* et al. [44] Based on this, no widespread hydrophobic patches can be found, which implies that in case of adsorption on carriers with rather lipophilic properties, there is no preferred orientation for the immobilization of hTH. Toward electrostatically charged surfaces hTH shows extensive areas displaying both negative or positive surface electrostatics (Fig. 8B, prepared with PDB2PQR webserver [45]). It can be reasoned that MNP—Am, the carrier with the highest $pK_{a,base}$ value was able to create ionic interaction with the negative regions of hTH. It needs to be noted that the catalytic center of hTH is highly negatively charged as well. Theoretically it would be possible that the carrier interferes with the electrostatic properties of the center responsible for the enzymatic catalysis, however, our results showed that the MNP-Am is a suitable carrier for the immobilization of hTH. Lastly, covalent immobilization

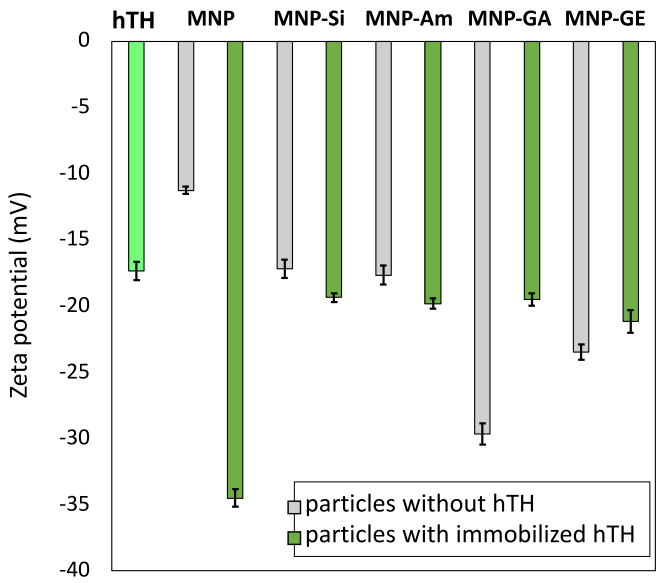

Fig. 6. Zeta potential of ■ native (non-immobilized) hTH, ■ magnetic nanoparticles without hTH (MNP: bare Fe_3O_4 particles, MNP—Si: MNP covered with silica shell built from TEOS, MNP—Am: amino-functionalized MNP—Si, MNP-GA: glutardialdehyde functionalized MNP—Am, MNP-GE: glycerol diglycidyl ether functionalized MNP—Am) and ■ hTH immobilized on MNPs. (For interpretation of the references to color in this figure legend, the reader is referred to the web version of this article.)

methods were exploited in the study as well, because potentially available Lys and Ser residues on the surface of hTH are able to form covalent bond with the linkers of MNP-GE or MNP-GA carriers. Fig. 8C shows the location and orientation of such residues, the zoomed in part shows where these residues are most abundant. According to this, hTH is basically able to establish covalent bonds in any direction, the final orientation is most probably directed by the lipophilic-lipophilic or dipole-dipole interactions between the carrier and the enzyme.

The effect on substrate amount on the specific enzyme activity was also investigated in case of the two significantly differ carriers with the highest U_E values, MNP-Am and MNP-GA. Similarly to native hTH, among the three relevant L-Tyr concentration (50, 100 and 200 μM), L-Tyr at 100 μM produced the largest U_E for both type of MNP carrier ($U_E = 13.9 \pm 2.2$ for 50 μM, $U_E = 48.3 \pm 32.6$ for 100 μM and $U_E = 5.0 \pm 2.6$ for 200 μM in case of MNP-Am and $U_E = 138.5 \pm 53.3$ for 50 μM, $U_E = 204.4 \pm 48.9$ for 100 μM and $U_E = 36.4 \pm 0.6$ for 200 μM in case of MNP-GA) see results in Fig.S6 in SI). This observation may lead to the conclusion that the immobilization procedure does not change the natural affinity of the enzyme.

3.5. *Operational and storage stability of hTH immobilized on onto magnetic nanoparticles with different surface linkers*

One of the potential applications of hTH could be the enzyme replacement therapy, where the hTH is taken from external sources to support the enzymatic deficiency related to L-DOPA production of human brain. Nasal adsorption could be a promising way applying spray-based nasal delivery of hTH immobilized on MNPs. The adsorption of drug containing nanoparticles is a common nasal formula and particles larger than 200 nm usually follow the so-called respiratory or the systemic pathway through the blood-brain-barrier (BBB) [46]. For the early-stage development of nasal formulation the stability of active compounds is usually investigated in simulated nasal electrolyte solution (SNES) [47]. Thus the operational stability of hTH immobilized on MNPs was investigated in SNES fluids (see details in Section 4.2 in SI). Results showed that hTH and all immobilized hTh are able to catalyze L-DOPA production in SNES fluid. Based on the results (Fig. 9.),

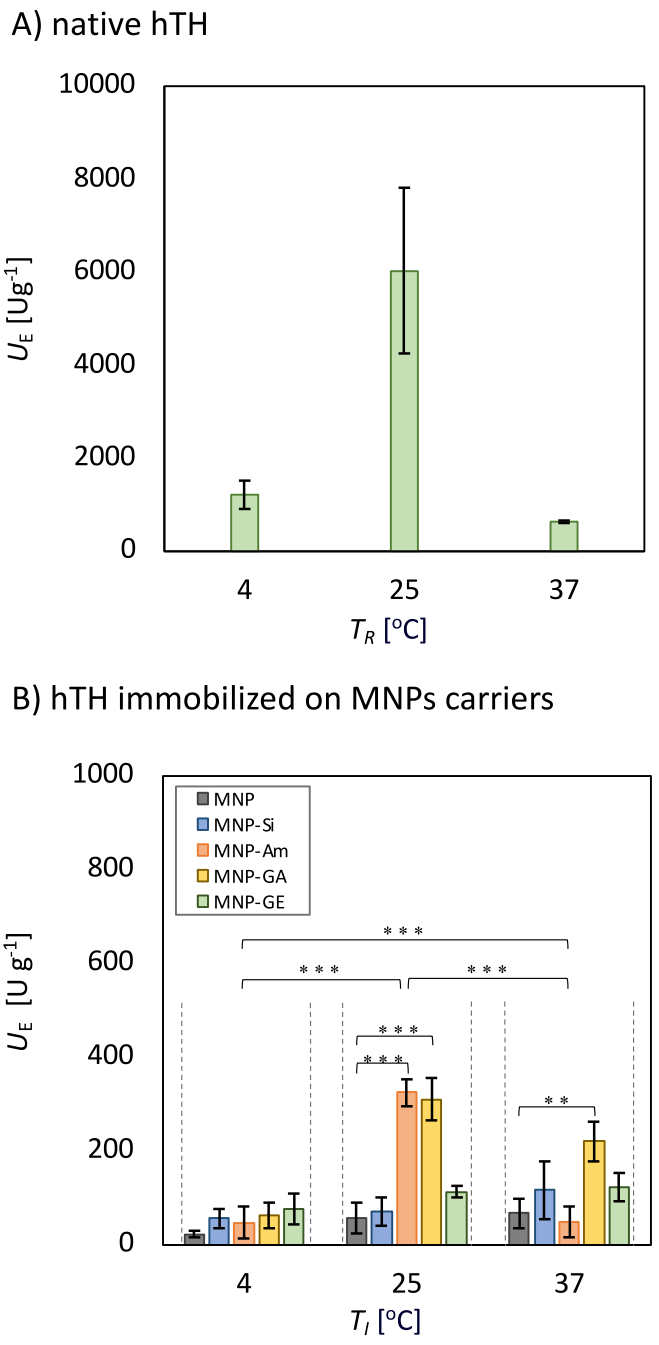

Fig. 7. Specific enzyme activity (U_E, Ug^{-1}) of A) native (non-immobilized) hTH incubated at different temperatures (4, 25 and 37 °C) for 1 h; and B) hTH immobilized on different magnetic nanoparticles (MNP: bare Fe_3O_4 particles, MNP—Si: MNP covered with silica shell, MNP—Am: amino-functionalized MNP—Si, MNP-GA: glutardialdehyde functionalized MNP—Am, MNP-GE: glycerol diglycidyl ether functionalized MNP—Am) at ■ 4 °C, ■ 25 °C and ■ 37 °C. Statistical analysis had been performed applying post hoc analysis, where asterisks indicating the significance levels (*p < 0.05, **p < 0.01, ***p < 0.001). (For interpretation of the references to color in this figure legend, the reader is referred to the web version of this article.)

independent *t*-tests were conducted, preceded by tests for normality (Shapiro-Wilk) and equality of variances (Brown-Forsythe). Results indicated no significant departure from normality or variance heterogeneity. Significant differences between the different linkers (Si, Am, GA and GE) and the reference MNP revealed by the t-tests, are denoted by * ($p < 0.05$) and ** ($p < 0.01$). However, significant difference could not be seen among the linkers, MNP—Si, MNP—Am, MNP-GA and MNP-GE

Table 1
Predicted physico-chemical parameters of MNPs surface linkers, MNP covered with silica shell (MNP—Si), MNP further functionalized with amino groups (MNP—Am), and MNPs additionally surface modified with either glutardialdehyde (MNP-GA) or glycerol diglycidyl ether (MNP-GE).

Surface linker	$pK_{a,base}$	log*P*	$logD_{pH6.8}$	n_{Rot}
MNP-Si[a]	–	−0.31	−0.31	2
MNP-Am	10.6	−0.50	−3.49	3
MNP-GA	8.8	−1.75	−3.86	9
MNP-GE	7.5	0.55	−0.15	8

[a] Mono-ethoxy linker.

provided similar specific enzyme activity (U_E), which means average of 25 % enzymatic recovery (ER) of the native enzyme.

Storage tests were also carried out, in which the residual activity of native hTH and hTH immobilized on MNP-Am or MNP-GA stored at 4 °C were compared after approximately two months. In case native hTH, high amount of solid precipitants appeared, making it impossible to accurately determine the protein content and enzymatic activity. This finding is consistent with previous studies published in the literature [19,48]. Due to the immobilization of hTH on to magnetic nanoparticles hTH preparations conserved the enzymatic activity, because the residual activity (RU_E) was 22.0 ± 2.9 % for MNP-Am and RU_E is 33.2 ± 2.8 % for MNP-GA (see results in fig.S7). The results suggest that the immobilization could protect the enzyme from deactivation and this benefit was greater in the case of covalent attachment (by MNP-GA) than the binding via ionic interactions (by MNP—Am).

4. Conclusion

In this work, hTH was immobilized on a variety of MNPs for the first time. The Raman mapping confirmed that all carriers were able to bind hTH on their surface homogenously. Immobilization yield and enzymatic activity measurements showed that the binding ability of the carriers varied significantly, and that the catalytic activity of the enzyme was greatly influenced by the means of immobilization. The analysis of the physico-chemical parameters of the different surface linkers indicated, that the surface of the MNP-Am carrier is mostly covered with positively charged ammonium groups that are able to interact with the negatively charged patches of hTH. This gentle interaction (opposing the covalent attachment formed in case of MNP-GA and MNP-GE carriers) proved to be the best from the five tested surface modifications for the fixation of catalytically active conformation of hTH.

Our work introduces the magnetic nanoparticles as potential tool for the optimization of hTH immobilization. On one hand, MNP carrier could be applied as formulation excipients or smart delivery systems for hTH-based therapies with controllable position and residence time. Furthermore, MNPs allow rapid, easy, and comprehensive investigations about enzyme immobilization, providing essential information about the optimal binding properties of hTH, which could lead to a stable and active form of the hTH. Regarding the potential application of hTH such as enzyme replacement therapies the formulation and immobilization of the enzyme is inevitable. Our result showed that magnetic nanoparticles with covalent binding linkers such as glutardialdehyde (MNP-GA) or glycerol diglycidyl ether (MNP-GE) are able to the irreversible immobilization of hTH and at the relevant temperature (37 °C) for human in vivo application, these carriers could ensure remarkable enzymatic recovery (ER) of the native hTH (ER = 38.1 % for MNP-GA and ER = 16.5 % for MNP-GE). The operational stability of immobilized hTH was also investigated in simulated nasal electrolyte fluid (SENS) to simulate the condition of nasal uptake. The ER of hTH bounded on modified MNPs was in the range of 17–27 %, which could be considered as promising

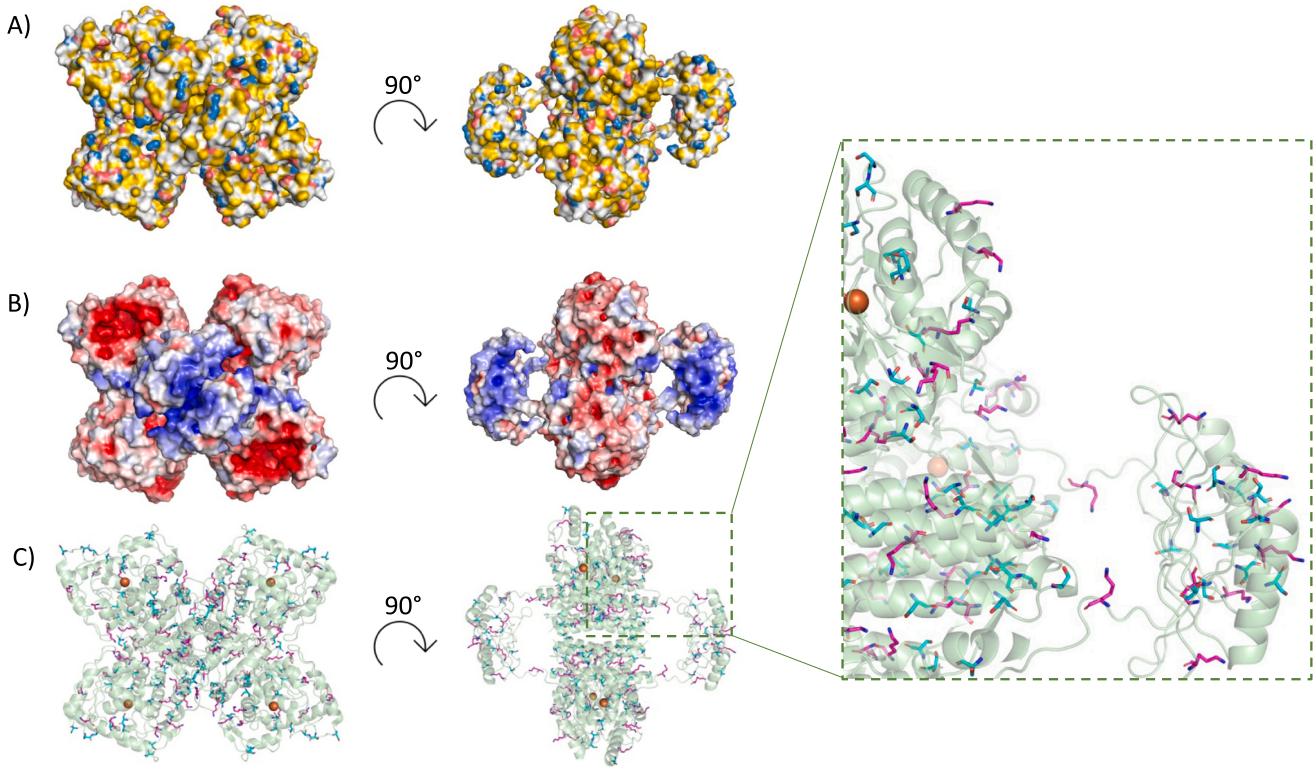

Fig. 8. Structure of hTH (PDB ID: 7A2G) with different visualization. A) Hydrophobicity pattern of hTH, (coloring: hydrocarbon groups without polar substitutions, yellow; negatively charged oxygens of glutamate and aspartate, red; nitrogens of positively charged functional groups of lysine and arginine, blue; all remaining atoms including the polar backbone, white). B) Surface electrostatic potential of hTH. C) Cartoon representation of hTH, Lys and Ser residues are highlighted (with magenta and cyan, respectively), as residues capable of forming covalent bonds with epoxide and aldehyde groups. (For interpretation of the references to color in this figure legend, the reader is referred to the web version of this article.)

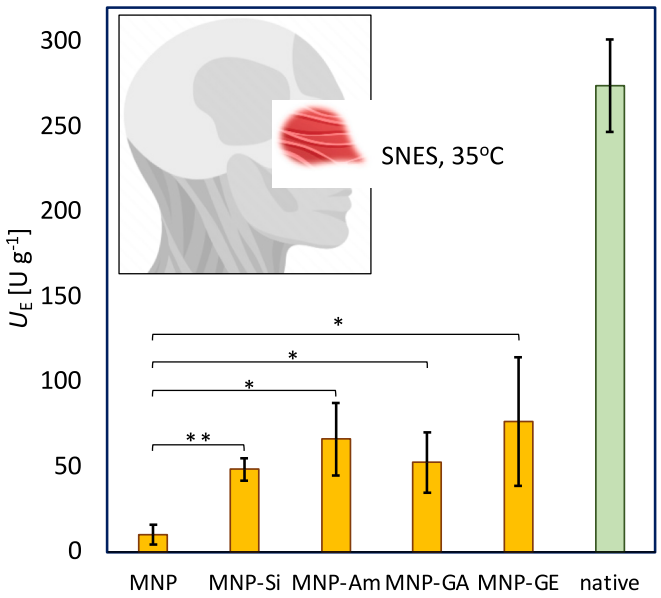

Fig. 9. Specific enzyme activity (U_E, Ug^{-1}) of native (non-immobilized) hTH and hTH immobilized on different magnetic nanoparticles (MNP: bare Fe_3O_4 particles, MNP—Si: MNP covered with silica shell, MNP—Am: amino-functionalized MNP—Si, MNP-GA: glutardialdehyde functionalized MNP—Am, MNP-GE: glycerol diglycidyl ether functionalized MNP—Am) in simulated nasal electrolyte solution (SNES) at 35 °C in one-hour time frame. Statistical analysis had been performed applying post hoc analysis, where asterisks indicating the significance levels (*p < 0.05, **p < 0.01.

results. Stability test performed after two months of storage at 4 °C showed that hTH immobilized on MNPs via ionic (MNP—Am) and covalent forces (MNP-GA) had residual activity >20 and 30 % respectively. However, these findings are promising, the enzymatic recovery may need further optimization, necessitating a thorough analysis of binding linkers. Regarding the nasal administration of hTH-MNP complexes the cellular uptake may pose challenges and may require further modification particle morphology and surface of the particles, to achieve the proper biological action. Overall, our study shows a multidisciplinary approach on the investigation of enzyme-carrier interactions. Expectedly, these results will support further research in the field of enzyme stabilization, especially for sensitive enzymes. In addition, immobilization of hTH onto nanocarriers could open new opportunities in enzyme-based therapies as well.

Funding

This research has been supported by the National Research Development and Innovation Office (NRDI) Fund via grant FK-137582 (D.B. W.), K-119493 (B.G.V.) and K-135231 (B.G.V.). D.B.W. also acknowledges the János Bolyai Research Scholarship of the Hungarian Academy of Sciences (BO/00175/21). The authors acknowledge the Project no. TKP-6-6/PALY-2021 has been implemented with the support provided by the Ministry of Culture and Innovation of Hungary from the National Research, Development and Innovation Fund, financed under the TKP2021-NVA funding scheme. The support of ÚNKP-22-4-II-BME-158 (Z.M.) and ÚNKP-23-5-BME-430 (D.B.W.) has been acknowledged. The research has been supported by Project RRF-2.3.1-21-2022-000 15, which has been implemented with the support provided by the European Union.

CRediT authorship contribution statement

Zsófia Molnár: Software, Methodology, Investigation, Conceptualization. **Réka Farkas:** Investigation. **Noémi Péli:** Investigation. **Balázs Decsi:** Methodology, Investigation. **Gábor Katona:** Writing – original draft, Visualization, Methodology, Investigation. **György T. Balogh:** Methodology, Investigation, Conceptualization. **Beáta G. Vértessy:** Methodology, Conceptualization. **Diána Balogh-Weiser:** Writing – review & editing, Visualization, Supervision, Resources, Methodology, Conceptualization.

Declaration of competing interest

The authors declare that they have no known competing financial interests or personal relationships that could have appeared to influence the work reported in this paper.

Acknowledgment

We would like to thank Prof. Dr. Aurora Martinez (University of Bergen) and Dr. Marte Flydal that their kindly gifted plasmids in the beginning of our work.

Appendix A. Supplementary data

Supplementary data to this article can be found online at https://doi.org/10.1016/j.ijbiomac.2024.131939.

References

[1] K. Waløen, R. Kleppe, A. Martinez, J. Haavik, Tyrosine and tryptophan hydroxylases as therapeutic targets in human disease, Expert Opin. Ther. Targets 21 (2017) 167–180, https://doi.org/10.1080/14728222.2017.1272581.
[2] K.M. Roberts, P.F. Fitzpatrick, Mechanisms of tryptophan and tyrosine hydroxylase, IUBMB Life 65 (2013) 350–357, https://doi.org/10.1002/iub.1144.
[3] A. Groaz, S. Galvan, L. Valer, D. Rossetto, F. Benedetti, G. Guella, Ö.D. Toparlak, S. S. Mansy, Cell-free synthesis of dopamine and serotonin in two steps with purified enzymes, Adv. Biosyst. 2000118 (2020) 2–6, https://doi.org/10.1002/adbi.202000118.
[4] Y. Satoh, K. Tajima, M. Munekata, J.D. Keasling, T.S. Lee, Engineering of L-tyrosine oxidation in Escherichia coli and microbial production of hydroxytyrosol, Metab. Eng. 14 (2012) 603–610, https://doi.org/10.1016/j.ymben.2012.08.002.
[5] P. Peralta-Yahya, A.M. Ehrenworth, Pterin-dependent biocatalysis and uses thereof, WO2016109769A1, https://patents.google.com/patent/WO2016109769A1/en#patentCitations, 2016.
[6] M.T. Bueno-Carrasco, J. Cuéllar, M.I. Flydal, C. Santiago, T. Kråkenes, R. Kleppe, J. R. López-blanco, M. Marcilla, K. Teigen, S. Alvira, P. Chacón, A. Martinez, J. M. Valpuesta, Structural mechanism for tyrosine hydroxylase inhibition by dopamine and reactivation by Ser40 phosphorylation, Nat. Commun. 13 (2022) 1–16, https://doi.org/10.1038/s41467-021-27657-y.
[7] B. Almas, B. Le Bourdelles, T. Flatmark, J. Mallet, J. Haavik, Regulation of recombinant human tyrosine hydroxylase isozymes by catecholamine binding and phosphorylation Structurelactivity studies and mechanistic implications, Eur. J. Biochem. 209 (1992) 249–255, https://doi.org/10.1111/j.1432-1033.1992.tb17283.x.
[8] P.W. Dickson, G.D. Briggs, Tyrosine hydroxylase. Regulation by feedback inhibition and phosphorylation, in: Adv. Pharmacol, 1st ed., Elsevier Inc., 2013, pp. 13–21, https://doi.org/10.1016/B978-0-12-411512-5.00002-6.
[9] I.T. Lehmann, L. Bobrovskaya, S.L. Gordon, P.R. Dunkley, P.W. Dickson, Differential regulation of the human tyrosine hydroxylase isoforms via hierarchical phosphorylation, J. Biol. Chem. 281 (2006) 17644–17651, https://doi.org/10.1074/jbc.M512194200.
[10] K.E. Goodwill, C. Sabatier, C. Marks, R. Raag, P.F. Fitzpatrick, R.C. Stevens, Crystal structure of tyrosine hydroxylase at 2.3 Å and its implications for inherited neurodegenerative diseases, Nat. Struct. Biol. 4 (1997) 578–585, https://doi.org/10.1038/nsb0797-578.
[11] P.J. Hillas, P.F. Fitzpatrick, A mechanism for hydroxylation by tyrosine hydroxylase based on partitioning of substituted phenylalanines, Biochemistry 35 (1996) 6969–6975, https://doi.org/10.1021/bi9606861.
[12] P.F. Fitzpatrick, Tetrahydropterin-dependent amino acid hydroxylases, Annu. Rev. Biochem. 68 (1999) 355–381, https://doi.org/10.1146/annurev.biochem.68.1.355.
[13] P.D. Szigetvari, G. Muruganandam, J.P. Kallio, E.I. Hallin, A. Fossbakk, R. Loris, I. Kursula, L.B. Møller, P.M. Knappskog, P. Kursula, J. Haavik, The quaternary structure of human tyrosine hydroxylase: effects of dystonia-associated missense variants on oligomeric state and enzyme activity, J. Neurochem. 148 (2019) 291–306, https://doi.org/10.1111/jnc.14624.
[14] T. Nagatsu, A. Nakashima, H. Ichinose, K. Kobayashi, Human tyrosine hydroxylase in Parkinson's disease and in related disorders, J. Neural Transm. 126 (2019) 397–409, https://doi.org/10.1007/s00702-018-1903-3.
[15] G. Nygaard, P.D. Szigetvari, A.K. Grindheim, P. Ruoff, A. Martinez, J. Haavik, R. Kleppe, M.I. Flydal, Personalized medicine to improve treatment of dopa-

responsive dystonia — a focus on tyrosine hydroxylase deficiency, J. Pers. Med. 11 (2021) 1–28.
[16] T. Nagatsu, M. Sawada, L-dopa therapy for Parkinson's disease: past, present, and future, Parkinsonism Relat. Disord. 1 (2009) 3–8, https://doi.org/10.1016/S1353-8020(09)70004-5.
[17] A. Willemsen, M.M. Verbeek, E. Kamsteeg, J.F.D.R. Andel, A. Aeby, N. Blau, A. Burlina, M.A. Donati, B. Geurtz, P.J. Grattan-smith, M. Haeussler, G. F. Hoffmann, H. Jung, P. De Lonlay, A. Megarbane, H. Monaghan, W.O. Renier, P. Rondot, J.A. Smeitink, G.C. Steenbergen-spanjers, M.M. Ryan, D.I. Zafeiriou, R. A. Wevers, Tyrosine hydroxylase deficiency: a treatable disorder of brain catecholamine biosynthesis, Brain 133 (2010) 1810–1822, https://doi.org/10.1093/brain/awq087.
[18] W.M. Pardridge, Tyrosine hydroxylase replacement in experimental Parkinson's disease with transvascular, Gene Ther. 2 (2005) 129–138.
[19] M.T. Bezem, F.G. Johannessen, K. Jung-Kc, E.T. Gundersen, A. Jorge-Finnigan, M. Ying, D. Betbeder, L. Herfindal, A. Martinez, Stabilization of human tyrosine hydroxylase in maltodextrin nanoparticles for delivery to neuronal cells and tissue, Bioconjug. Chem. 29 (2018) 493–502, https://doi.org/10.1021/acs.bioconjchem.7b00807.
[20] M.T. Bezem, F.G. Johannessen, T. Kråkenes, M.J. Sailor, A. Martinez, Relevance of electrostatics for the interaction of tyrosine hydroxylase with porous silicon nanoparticles, Mol. Pharm. 18 (2021) 976–985, https://doi.org/10.1021/acs.molpharmaceut.0c00960.
[21] M. Bilal, Y. Zhao, T. Rasheed, H.M.N. Iqbal, Magnetic nanoparticles as versatile carriers for enzymes immobilization: a review, Int. J. Biol. Macromol. 120 (2018) 2530–2544, https://doi.org/10.1016/j.ijbiomac.2018.09.025.
[22] A.G. Niculescu, C. Chircov, A.M. Grumezescu, Magnetite nanoparticles: synthesis methods – a comparative review, Methods 199 (2022) 16–27, https://doi.org/10.1016/J.YMETH.2021.04.018.
[23] H. Wu, W. Mu, Application prospects and opportunities of inorganic nanomaterials for enzyme immobilization in the food-processing industry, Curr. Opin. Food Sci. 47 (2022) 100909, https://doi.org/10.1016/J.COFS.2022.100909.
[24] R.A. Bohara, N.D. Thorat, S.H. Pawar, Role of functionalization: strategies to explore potential nano-bio applications of magnetic nanoparticles, RSC Adv. 6 (2016) 43989–44012, https://doi.org/10.1039/C6RA02129H.
[25] H.M. Williams, H. Price, The application of magnetic nanoparticles in the treatment and monitoring of cancer and infectious diseases, Biosci. Horizons Int. J. Student Res. 10 (2017) 2017, https://doi.org/10.1093/BIOHORIZONS/HZX009.
[26] B. Socas-Rodríguez, A.V. Herrera-Herrera, M. Asensio-Ramos, M.Á. Rodríguez-Delgado, et al., Process 8 (2020) 1140, https://doi.org/10.3390/PR8091140.
[27] X. Yu, T. Zhong, Y. Zhang, X. Zhao, Y. Xiao, L. Wang, X. Liu, X. Zhang, Design, preparation, and application of magnetic nanoparticles for food safety analysis: a review of recent advances, J. Agric. Food Chem. 70 (2022) 46–62, https://doi.org/10.1021/acs.jafc.1c03675.
[28] M.A. Busquets, A. Espargaro, R. Sabaté, J. Estelrich, Magnetic nanoparticles cross the blood-brain barrier: when physics rises to a challenge, Nanomaterials 5 (2015) 2231–2248, https://doi.org/10.3390/nano5042231.
[29] R. Qiao, Q. Jia, S. Hüwel, R. Xia, T. Liu, F. Gao, H.-J. Galla, M. Gao, Receptor-mediated delivery of magnetic nanoparticles across the blood-brain barrier, ACS Nano 5 (2012) 3304–3310.
[30] L.B. Thomsen, M.S. Thomsen, T. Moos, Targeted drug delivery to the brain using magnetic nanoparticles, Ther. Deliv. 6 (2015) 1145–1155, https://doi.org/10.4155/tde.15.56.
[31] A.A. Gkountas, N.D. Polychronopoulos, G.N. Sofiadis, E.G. Karvelas, L.A. Spyrou, I. E. Sarris, Simulation of magnetic nanoparticles crossing through a simplified blood-brain barrier model for glioblastoma multiforme treatment, Comput. Methods Programs Biomed. 212 (2021) 106477, https://doi.org/10.1016/j.cmpb.2021.106477.
[32] J. Chen, M. Yuan, C.A. Madison, S. Eitan, Y. Wang, Blood-brain barrier crossing using magnetic stimulated nanoparticles, J. Control. Release 345 (2022) 557–571, https://doi.org/10.1016/j.jconrel.2022.03.007.
[33] J.O. Morales, P.J.G. Editor, W. Walz, Nanomedicines for Brain Drug Delivery, Humana Press, 2021.
[34] M.E. Johnson, M.F. Salvatore, S.A. Maiolo, L. Bobrovskaya, Tyrosine hydroxylase as a sentinel for central and peripheral tissue responses in Parkinson's progression: evidence from clinical studies and neurotoxin models, Prog. Neurobiol. 165–167 (2018) 1–25, https://doi.org/10.1016/j.pneurobio.2018.01.002.
[35] H. Thoenen, Induction of tyrosine hydroxylase in peripheral and central adrenergic neurones by cold-exposure of rats, Nature 228 (1970) 861–862, https://doi.org/10.1038/228861a0.
[36] L.M. Vermeer, C.A. Higgins, D.L. Roman, J.A. Doorn, Real-time monitoring of tyrosine hydroxylase activity using a plate reader assay, Anal. Biochem. 432 (2013) 11–15, https://doi.org/10.1016/j.ab.2012.09.005.
[37] C. Liu, Z. Teng, Q. Lu, R. Zhao, X. Yang, C. Tang, J. Liao, Aggregation kinetics and ζ-potential of soy protein during fractionation, Food Res. Int. 44 (2011) 1392–1400, https://doi.org/10.1016/j.foodres.2011.01.054.
[38] C.A. Ross, M.A. Poirier, Protein aggregation and neurodegenerative disease, Nat. Med. 10 (2004) 10–17, https://doi.org/10.1038/nm1066.
[39] A. Baumann, A. Jorge-Finnigan, K. Jung-Kc, A. Sauter, I. Horvath, L.A. Morozova-Roche, A. Martinez, Tyrosine hydroxylase binding to phospholipid membranes prompts its amyloid aggregation and compromises bilayer integrity, Sci. Rep. 6 (2016) 1–14, https://doi.org/10.1038/srep39488.
[40] M.I. Flydal, T.-A. Krakenes, M.D.S. Tai, M.P.A. Tran, K. Teigen, A. Martinez, Levalbuterol lowers the feedback inhibition by dopamine and delays misfolding and aggregation in tyrosine hydroxylase, Biochimie 183 (2021) 126–132, https://doi.org/10.1016/j.biochi.2020.12.002.
[41] B.J. Kirby, Micro-and Nanoscale Fluid Mechanics: Transport in Microfluidic Devices, Cambridge University Press, Cambridge, MA, USA, 2010.
[42] J. Chapman, A.E. Ismail, C.Z. Dinu, Industrial applications of enzymes: recent advances, techniques, and outlooks, Catalysts 8 (2018) 1–26, https://doi.org/10.3390/catal8060238.
[43] Y. Li, J.S. Church, A.L. Woodhead, Infrared and Raman spectroscopic studies on iron oxide magnetic nano-particles and their surface modifications, J. Magn. Magn. Mater. 324 (2012) 1543–1550, https://doi.org/10.1016/j.jmmm.2011.11.065.
[44] D. Hagemans, I.A.E.M. van Belzen, T.M. Luengo, S.G.D. Rüdiger, A script to highlight hydrophobicity and charge on protein surfaces, Front. Mol. Biosci. 2 (2015) 1–11, https://doi.org/10.3389/fmolb.2015.00056.
[45] T.J. Dolinsky, J.E. Nielsen, J.A. Mccammon, N.A. Baker, PDB2PQR: an automated pipeline for the setup of Poisson – Boltzmann electrostatics calculations, Nucleic Acids Res. 32 (2004) W665–W667, https://doi.org/10.1093/nar/gkh381.
[46] S.-H. Jeong, J.-H. Jang, Y.-B. Lee, Drug delivery to the brain via the nasal route of administration: exploration of key targets and major consideration factors, J. Pharm. Investig. 53 (2023) 119–152, https://doi.org/10.1007/s40005-022-00589-5.
[47] J. Castile, Y.H. Cheng, B. Simmons, M. Perelman, A. Smith, P. Watts, Development of in vitro models to demonstrate the ability of PecSys®, an in situ nasal gelling technology, to reduce nasal run-off and drip, Drug Dev. Ind. Pharm. 39 (2013) 816–824, https://doi.org/10.3109/03639045.2012.707210.
[48] M.T. Bezem, A. Baumann, L. Skjærven, R. Meyer, P. Kursula, A. Martinez, M. I. Flydal, Stable preparations of tyrosine hydroxylase provide the solution structure of the full-length enzyme, Sci. Rep. 6 (2016) 30390, https://doi.org/10.1038/srep30390.